A comprehensive study to determine spectral lines for CME diagnostics with current and future observatories

Yeimy Rivera, Enrico Landi, Susan T. Lepri

7th METIS Workshop 2019, Padova, Italy

November 12th 2019

solar orbiter

metis

DKIST
DANIEL K. INOUYE SOLAR TELESCOPE

Rivera, Y. J., Landi, E., Lepri, S. T., "Identifying spectral lines to study coronal mass ejection evolution in the lower corona", 2019, The Astrophysical Journal Supplement Series, 243, 34

Motivation

ACE

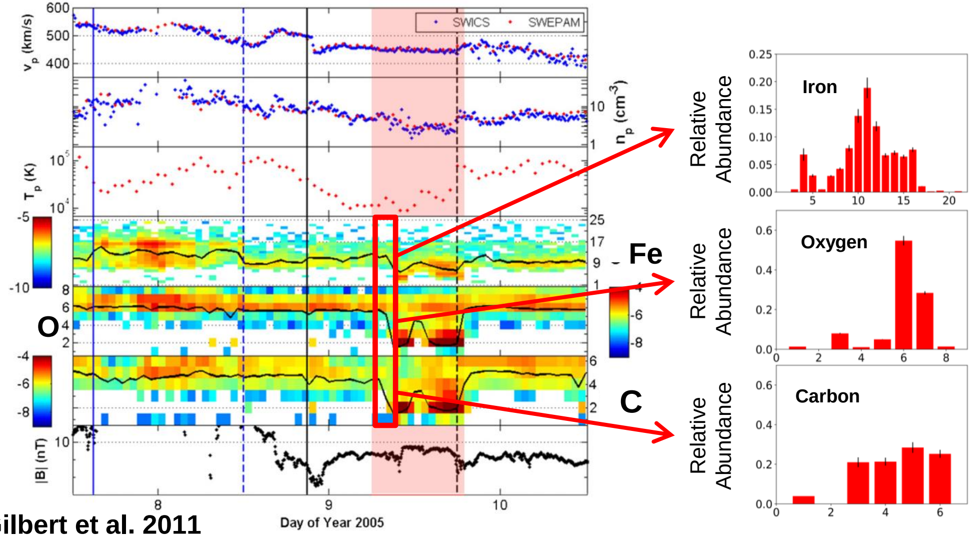

Gilbert et al. 2011

Rivera et al. 2019a

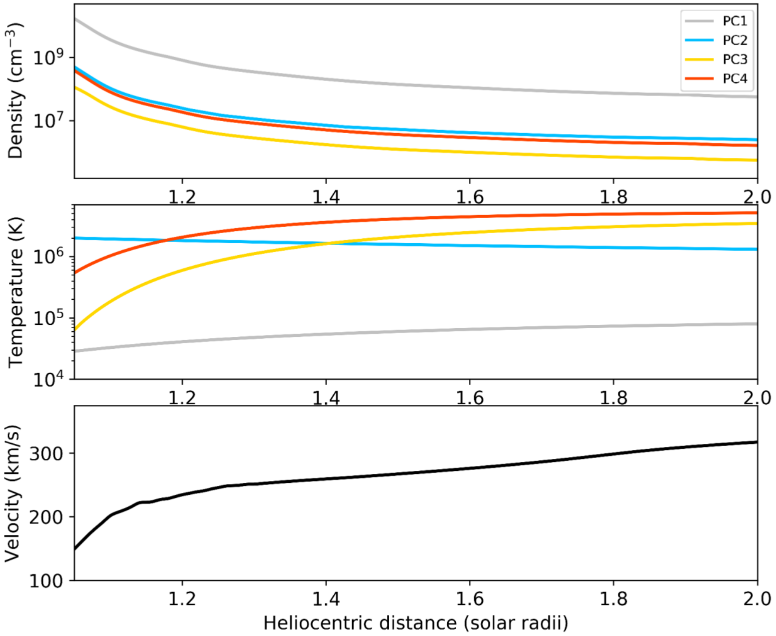

- Complex injection of energy and non uniform heating to adjacent CME structures
- Distinct thermal histories that cover a large range of temperatures and densities

Aim

- Anticipate line emission from CME plasma that will be useful to study the evolving prominence and adjacent structure through the corona
- Identify key lines
  - Prominent
  - Ionization equilibrium
  - Spectral range of current or planned instrumentation
    - DKIST
    - UCoMP ~ 2Rsun
    - SO/SPICE – 13 arcmin slit length and +/- 8 arcmin scan range
    - SO/METIS – 1.7Rs(min) - 9Rs(max)
- Proposal for future instrumentation

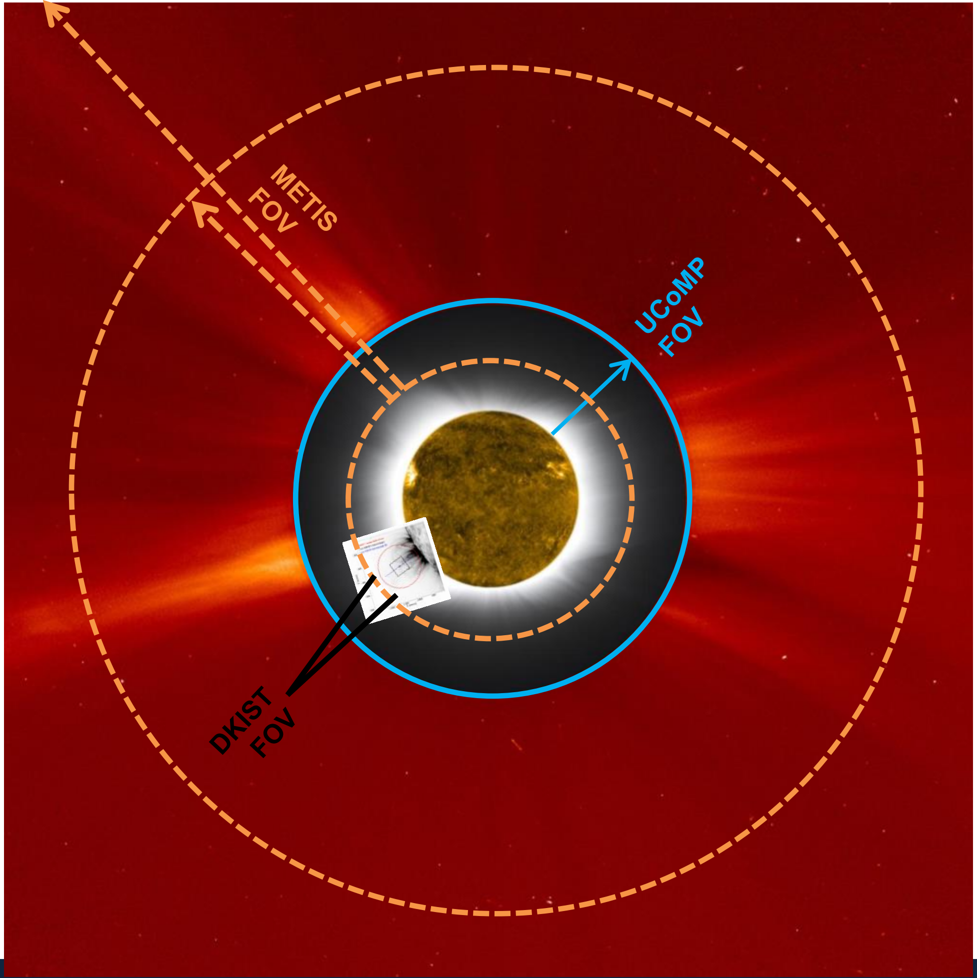

Upgraded Coronal Multichannel Polarimeter (UCoMP)

Coronagraph with multi-wavelength capability in the visible able to observe a nine spectrally resolved coronal lines over the entire corona out to $2R_{sun}$

Line (Å)	Ion	Temp (MK)
6564 (Hα)	H I	-
10830	**He I**	**-**
6373	Fe X	1.07
7894	Fe XI	1.26
10749	**Fe XIII**	**1.66**
10800	**Fe XIII**	**1.66**
5304	Fe XIV	2.00
6918	Ar XI	2.00
7062	Fe XV	2.19

Landi et al. 2016

Aim

- Anticipate line emission from CME plasma that will be useful to study the evolving prominence and adjacent structure through the corona
- Identify key lines
  - Prominent
  - Ionization equilibrium
  - Spectral range of current or planned instrumentation
    - DKIST
    - UCoMP ~ 2Rsun
    - SO/SPICE – 13 arcmin slit length and +/- 8 arcmin scan range
    - SO/METIS – 1.7Rs(min) - 9Rs(max)
- Proposal for future instrumentation

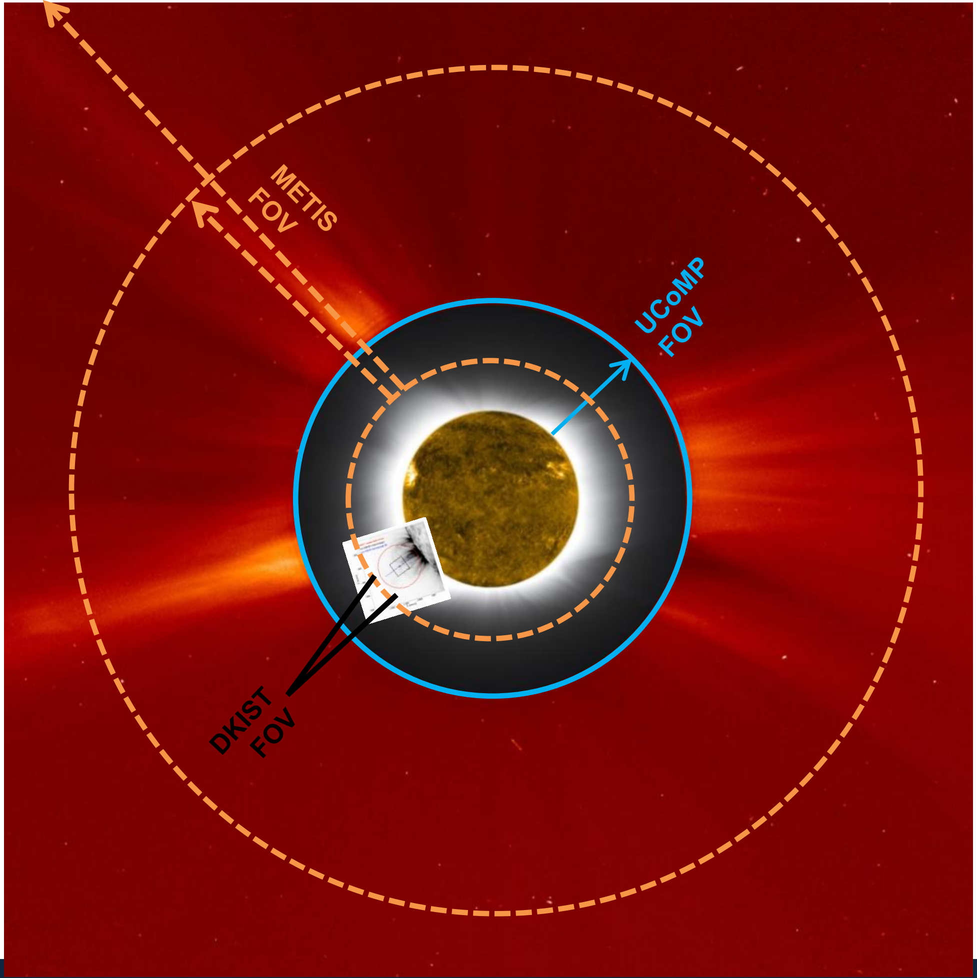

Candidate Spectral Lines

- How were they chosen?
  - Previously studied filament core (Landi et al. 2010)
    - EUV to near-infrared
    - Planned DKIST, SO/METIS and SO/SPICE spectral range
  - Test lines specific to UCoMP
- Lines tested: 118
- Ranges:
  - λ =100 - 14400 Å
  - Log T (K) = 4 - 6.7 (Chromospheric to sub-flare temperatures)

Table 2
A List of All the Lines Tested between 1001 and 4000 Å

Ion	λ (Å)	Log *T* (K)	Transition	Instrument Range
H I (Lyβ)	1025.72	⋯	$1s~^2S_{1/2}-3p~^2P_{1/2}$	×
H I (Lyα) METIS	1215.67	⋯	$1s~^2S_{1/2}-2p~^2P_{1/2}$	⋯
Ca II	3934.78	4.05	$3p^6~4s~^2S_{1/2}-3p^6~4p~^2P_{3/2}$	◊ (VBI blue)
S II	1259.52	4.25	$3s^2~3p^3~^4S_{3/2}-3s~3p^4~^4P_{5/2}$	⋯
C II	1036.34	4.40	$2s^2~2p~^2P_{1/2}-2s~2p^2~^2S_{1/2}$	×
C II	2748.09	4.40	$2s^2~3p~^2P_{3/2}-2s^2~4d~^2D_{5/2}$	⋯
N II	1083.99	4.45	$2s^2~2p^2~^3P_0-2s~2p^3~^3D_1$	⋯
O II	1128.07	4.45	$2s~2p^4~^4P_{5/2}-2s^2~2p^2~(3P)~3p~^4P_{5/2}$	⋯
Mg III	3354.70	4.55	$2s^2~2p^5~3d~^3P_0-2s^2~2p^5~4p~^3S_1$	⋯
Ne II	3345.36	4.55	$2s^2~2p^4~3s~^4P_{1/2}-2s^2~2p^4~3p~^4D_{1/2}$	⋯
S III	1190.20	4.70	$3s^2~3p^2~^3P_0-3s~3p^3~^3D_1$	⋯
Si III	1206.50	4.70	$3s^2~^1S_0-3s~3p~^1P_1$	⋯
Si III	1301.15	4.70	$3s~3p~^3P_1-3p^2~^3P_0$	⋯
Si III	1312.59	4.70	$3s~3p~^1P_1-3s~4s~^1S_0$	⋯
C III	1176.37	4.85	$2s~2p~^3P_2-2p^2~^3P_1$	⋯
N III	2248.65	4.85	$2s^2~3d~^2D_{5/2}-2s^2~4p~^2P_{3/2}$	⋯
N III	3366.77	4.85	$2s~2p~3s~^4P_{3/2}-2s~2p~3p~^4P_{1/2}$	⋯
O III	1153.78	4.90	$2s~2p^3~^3S_1-2p^4~^3P_2$	⋯
Fe V	3076.54	4.95	$3d^4~^3G_3-3d^4~(1)~^3F_2$	⋯
Fe V	3143.86	4.95	$3d^4~^3G_5-3d^4~(1)~^3F_4$	⋯
Fe V	3892.38	4.95	$3d^4~^5D_4-3d^4~(2)~^3F_4$	◊ (ViSP)
O IV	1338.62	5.15	$2s~2p^2~^2P_{1/2}-2p^3~^2D_{3/2}$	⋯
O IV	1399.78	5.15	$2s^2~2p~^2P_{1/2}-2s~2p^2~^4P_{1/2}$	⋯
O IV	1401.16	5.15	$2s^2~2p~^2P_{3/2}-2s~2p^2~^4D_{5/2}$	⋯
Fe VI	3814.63	5.20	$3p^6~3d^3~^4F_{3/2}-3p^6 3d^3~^2P_{3/2}$	◊ (ViSP)
Fe VI	3890.51	5.20	$3p^6~3d^3~^4F_{5/2}-3p^6~3d^3~^2P_{3/2}$	◊ (ViSP)
Fe VI	3983.44	5.20	$3p^6~3d^3~^2F_{5/2}-3p^6~3d^3~^2D_{5/2}$	◊ (ViSP)
O V	2790.67	5.35	$2s~3s~^3S_1-2s~3p~^3P_0$	⋯
Mg V	2783.58	5.45	$2s^2~2p^4~^3P_2-2s^2~2p^4~^1D_2$	⋯
O VI	1031.91	5.45	$1s^2~2s~^2S_{1/2}-1s^2~2p~^2P_{3/2}$	×
O VI	1037.61	5.45	$1s^2~2s~^2S_{1/2}-1s^2~2p~^2P_{1/2}$	×
Ne VI	1005.73	5.60	$2s^2~2p~^2P_{3/2}-2s~2p^2~^4P_{3/2}$	×
Mg VI	1190.12	5.65	$2s^2~2p^3~^4S_{3/2}-2s^2~2p^3~^2P_{3/2}$	⋯
Si VII	1049.15	5.79	$2s^2~2p^4~^3P_1-2s^2~2p^4~^1S_0$	⋯
Mg VIII	1075.81	5.90	$2s~2p^2~^2P_{3/2}-2p^3~^4S_{3/2}$	⋯
Fe X	1028.02	6.05	$3s2~3p^4~3d~^4D_{7/2}-3s^2~3p^4~3d~^2F_{7/2}$	×
Fe XIII	3388.91	6.25	$3s^2~3p^2~^3P_2-3s^2~3p^2~^1D_2$	⋯

Notes. "◊ ": planned DKIST range. "×": planned SO/SPICE range.

Synthetic Intensities

- Synthetic intensity as a function of distance
  - collisional excitation and radiative scattering using atomic data from CHIANTI
- Composition: Photospheric abundances from Asplund et al. (2009) and coronal abundances from Schmelz et al. (2012)

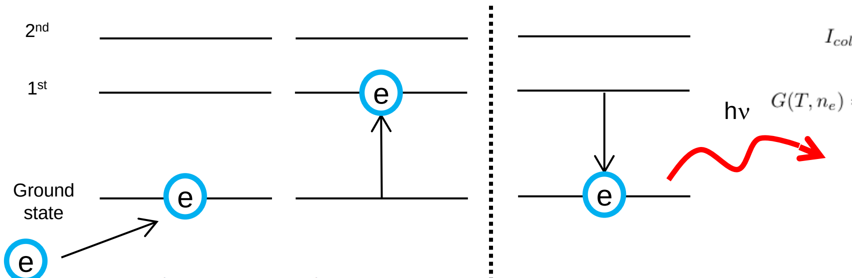

$$X_i^{+m} + e(E_1) \rightarrow X_j^{+m} + e(E_2)$$

$$X_j^{+m} \rightarrow X_k^{+m} + h\nu_{jk}$$

$$I_{coll} = \frac{1}{4\pi}\int_{-\infty}^{\infty} G(T,n_e)\varphi(T)dT$$

$$G(T,n_e) = \frac{n_j(X^{+q})}{n(X^{+q})}\frac{n(X^{+q})}{n(X)}\frac{n(X)}{n(H)}\frac{n(H)}{n_e}\frac{A_{ji}}{n_e}$$

$$\varphi(T) = n_e^2\frac{dx}{dT}$$

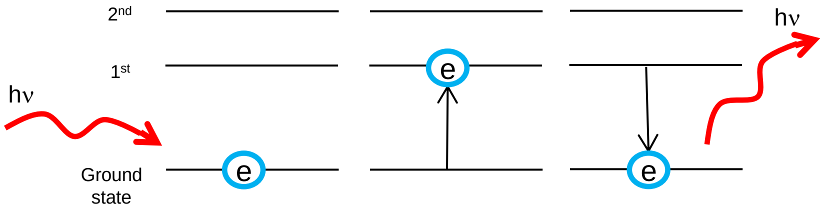

$$X_i^{+m} + h\nu_{ij} \rightarrow X_j^{+m}$$

$$X_j^{+m} \rightarrow X_i^{+m} + h\nu_{ji}$$

Spontaneous absorption/emission (B/A) coefficient

Scattering factor

Incident flux

$$I_{rad} = \frac{BA_{ij}}{4\pi A_{tot}}\int_{-\infty}^{\infty} N_{abs}p(\phi)F_{inc}D(v)dx$$

$$D(v) = \int_0^{\infty}\varphi(\nu_i)\psi(\nu_1,\nu)d\nu_1$$

$$N_{abs} = \frac{n(X^{+q})}{n(X)}\frac{n(X)}{n(H)}\frac{n(H)}{n_e}n_e$$

Doppler Dimming term

Number of absorbers

Synthetic Intensities

- Synthetic intensity as a function of distance
  - collisional excitation and radiative scattering using atomic data from CHIANTI
- Composition: Photospheric abundances from Asplund et al. (2009) and coronal abundances from Schmelz et al. (2012)
- Relative Abundances:
  - Within the evolution of the plasma from Michigan Ionization Code (Landi et al. 2010)
    - Input: Density, Temperature, Velocity
    - Output: **Relative abundances**

MIC Output

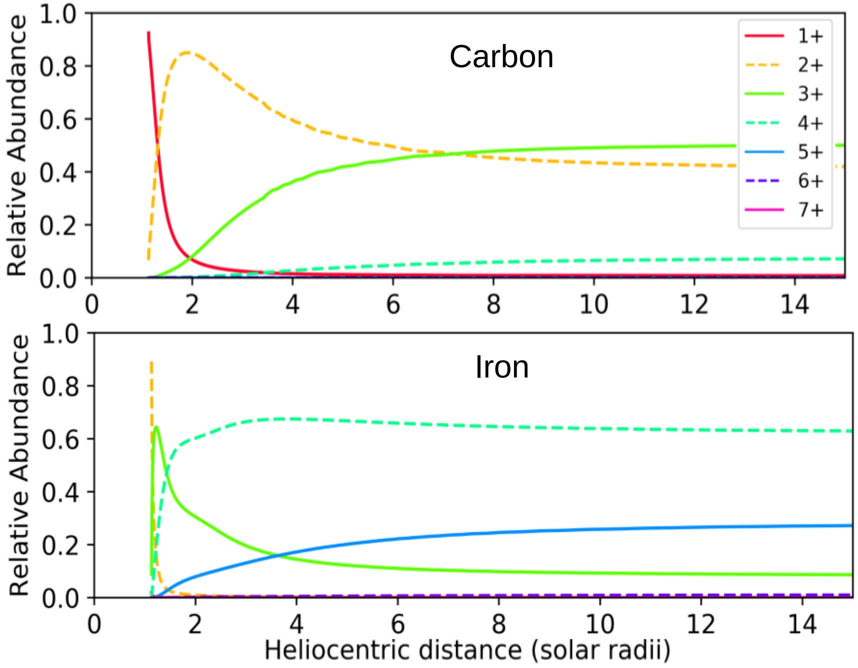

Rivera et al. 2019a

Synthetic Intensities

- Synthetic intensity as a function of distance
  - collisional excitation and radiative scattering using atomic data from CHIANTI
- Composition: Photospheric abundances from Asplund et al. (2009) and coronal abundances from Schmelz et al. (2012)
- Relative Abundances:
  - Within the evolution of the plasma from Michigan Ionization Code (Landi et al. 2010)
    - Input: Density, Temperature, Velocity
    - Output: **Relative abundances**
- Angular width, ϕ
- Filling factor
  - Prominence – 0.1-0.001 (Labrosse et al. 2010)

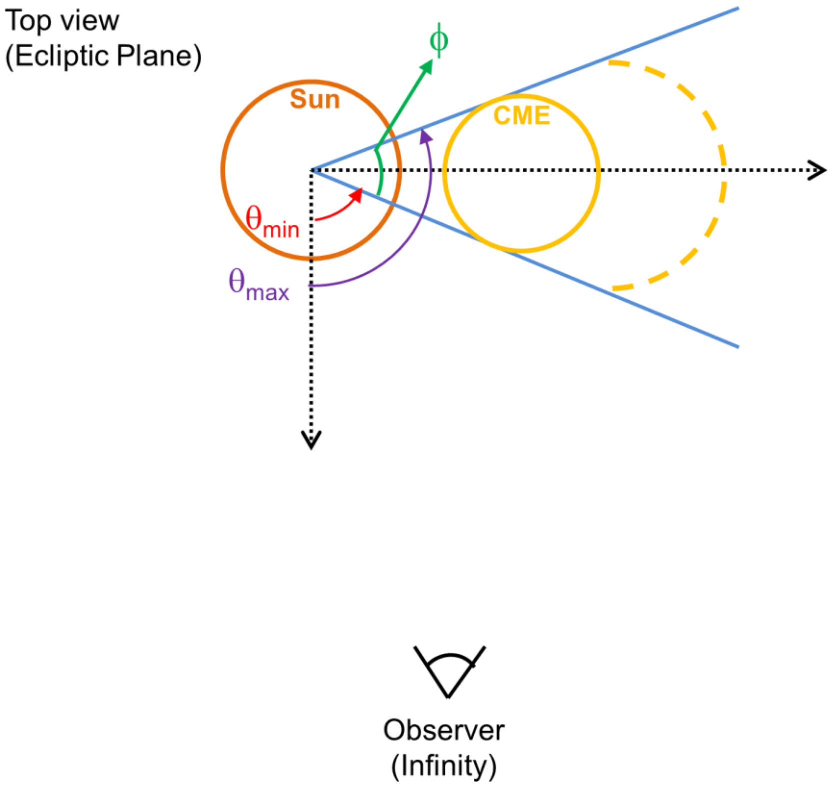

Plasma Evolution

Rivera et al. 2019a

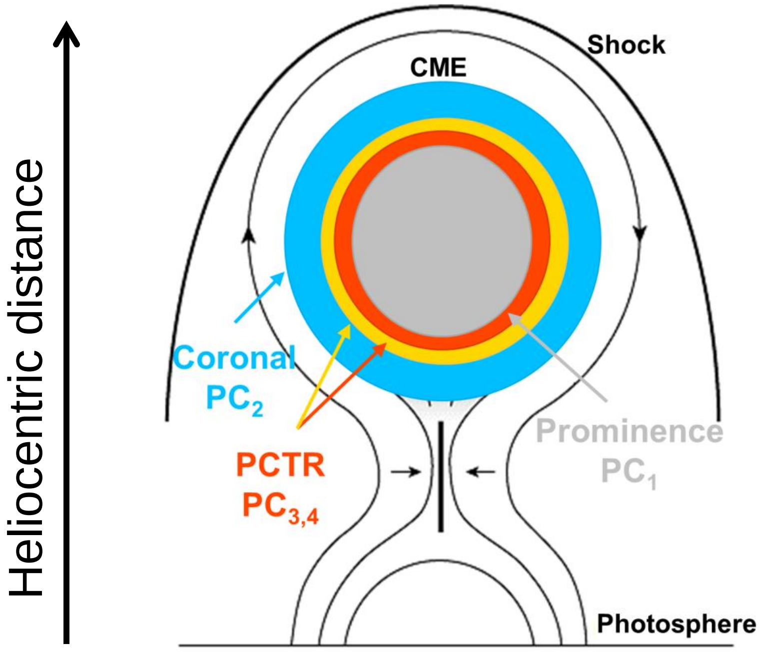

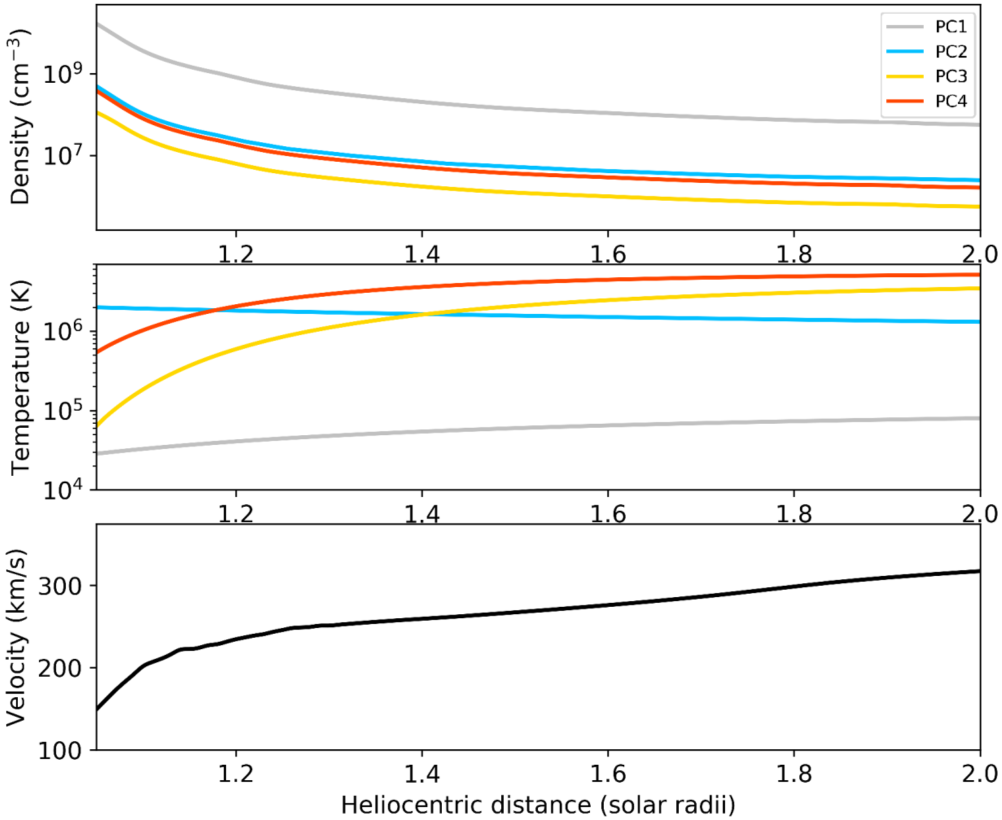

Synthetic Intensity – prominence

- Prominence produces brightest lines
- Intensities decrease sharply after leaving the surface
- Intensities generated match equilibrium intensities

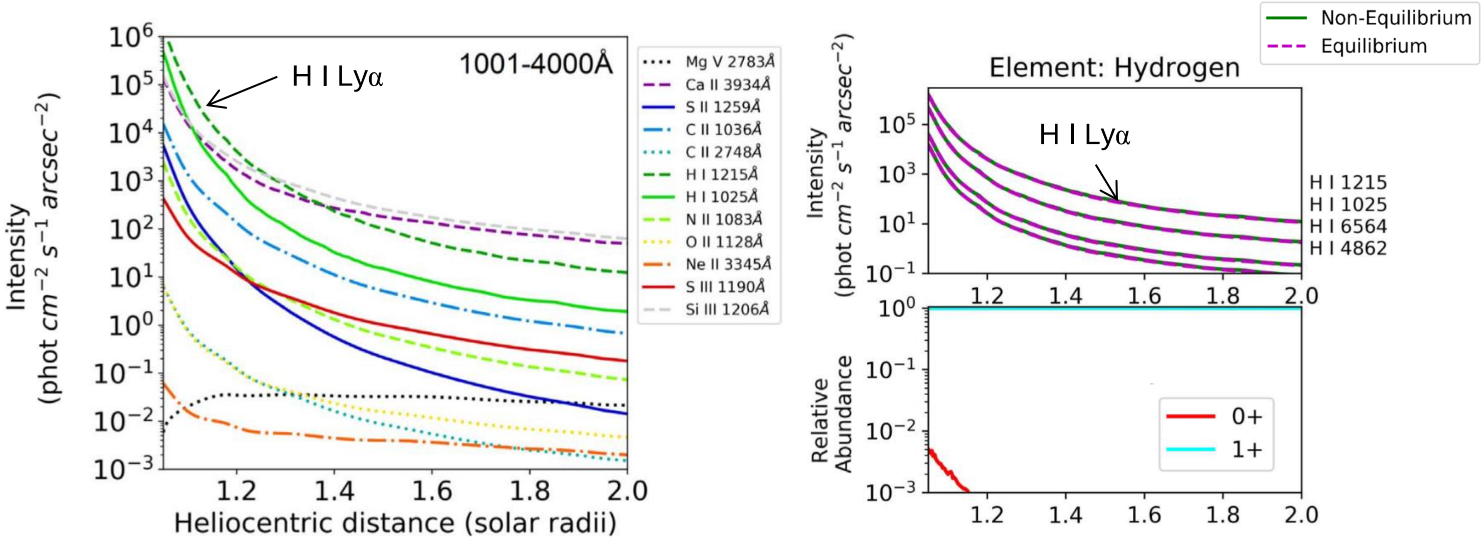

Filament core

ϕ=30° , ff = 0.1

Solar C III ⟶ Helio C^{2+}

Rivera et al. 2019b

Synthetic Intensity – prominence-coronal transition region

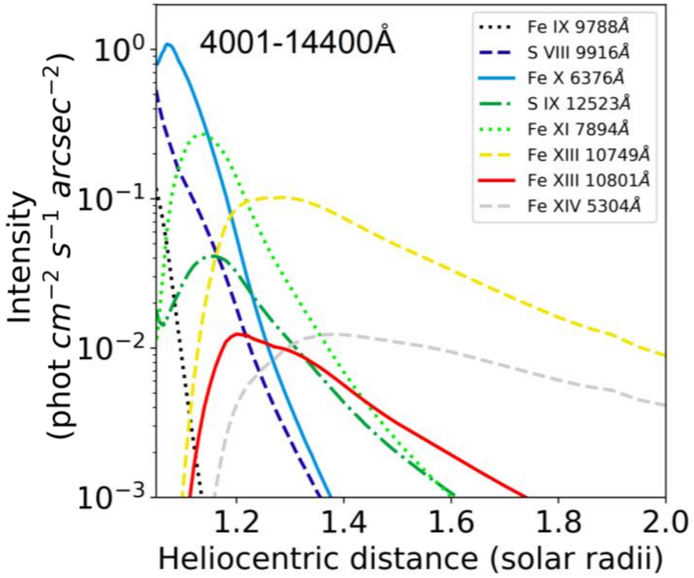

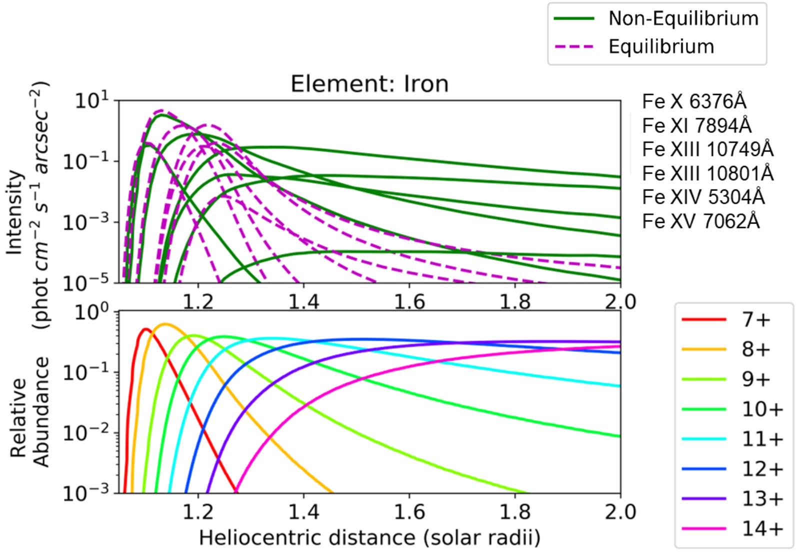

Prominence-Coronal
Transition Region
ϕ=5°, ff = 0.1

Rivera et al. 2019b

Synthetic Intensity – coronal plasma

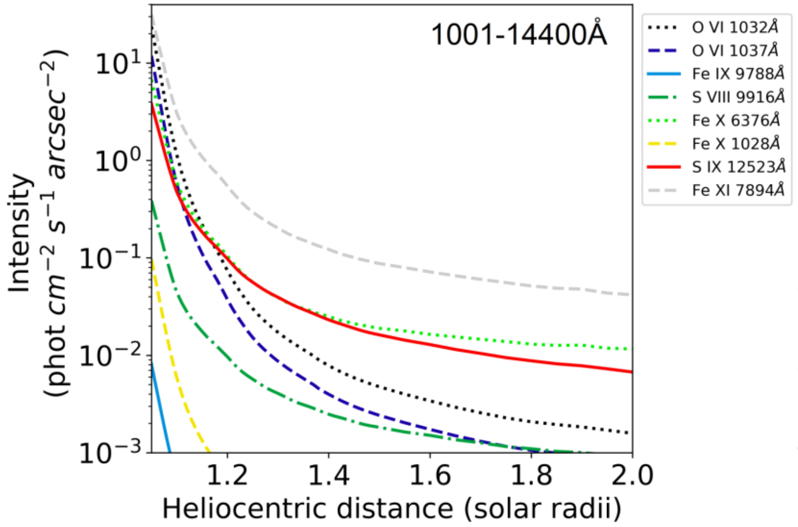

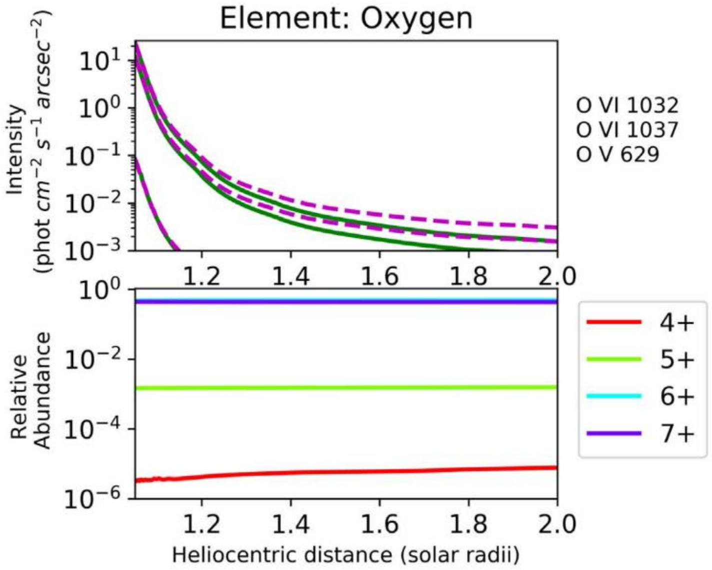

Coronal
ϕ=5°, ff = 1

Rivera et al. 2019b

Diagnostics - prominence plasma

Multiple same ion lines can be used for temperature/density diagnostics (need to check optical thickness for lines formed below ~log T (K) = 5.0)

> **N_e diagnostics:** N IV 923/765 and Si III 1312/1301
> **T_e diagnostics:** O III 702/599, O IV 790/553, and N III 991/686
> (Keenan & Aggarwal 1989; Wilhelm et al. 1995 and references therein)

METIS: **Lyα 1215**

UCoMP: **H I (Hα) 6564** and **He I 10830**

DKIST: **Ca II 8544** and **Hβ (4862)** pressure diagnostics of filaments (Heasley & Milkey 1978; Gouttebroze et al. 2002)

Ion	**Ratio**	**N_e (cm^{-3}) range**	**T_e (K) range**	**Instrument**
N IV	923/765	10^9-10^{11}	$1.4x10^5$	SO/SPICE
Si III	**1312/1301**	**10^9-10^{11}**	**$3.5x10^4$**	**SUMER**
O III	702/599		$10^{4.4}$-$10^{5.4}$	CDS/SOHO
O IV	790/553		$8x10^4$-$2x10^5$	CDS/SOHO SO/SPICE
N III	991/686		<$7x10^4$	SO/SPICE

Diagnostics - Coronal plasma

Multiple consecutive lines

Fe X, XI, XIV, and XV, which range in formation temperatures between 1 and 2.25 MK, can be useful to investigate heating throughout the plasma's 1.5R_{sun} evolution

Ar XI ~5 million K

UCoMP lines

Ion	Line (Å)	log Temp (K)
H I (Hα)	6564	-
He I	10830	-
Fe X	**6373**	**6.05**
Fe XI	**7894**	**6.12**
Fe XIII	**10749**	**6.25**
Fe XIII	**10800**	**6.25**
Fe XIV	**5304**	**6.30**
Fe XV	**7062**	**6.35**
Ar XI	**6918**	**6.68**

DKIST - Cryo-NIRSP

Si X	**14300**	**6.15**

Final Remarks

- We envision the lines will **facilitate complementary observations** between future instruments
- The recommended lines can be useful to **build comprehensive use-cases** with upcoming instruments available to study CMEs
- CME components can by studied with different instruments which can be combined to:
  - **study early stages of plasma evolution** with remote sensing observations
  - **connect with *in situ* observation on PSP and SO** while in quadrature with the earth

1. **Rivera, Y. J., Landi, E., Lepri, S. T., & Gilbert, J. A., 2019a, 583 The Astrophysical Journal, 874, 164**
2. **Rivera, Y. J., Landi, E., Lepri, S. T., 2019b, The Astrophysical Journal Supplement Series, 243, 34**

Table 1. Recommended lines above 1 phot cm^{-2} s^{-1} arcsec^{-2}.

Ion	λ (Å)	Log T (K)	Plasma Structure
H I (Ly-β)	1025.72	–	P
H I (Ly-α)	1215.67	–	P
H I (Hβ)	4862.73	–	P
H I (Hα)	6564.72	–	P
He I	4472.73	–	P
He I	5877.25	–	P
He I	7067.14	–	P
He I	10833.31	–	P
Ca II	3934.78	4.05	P
Ca II	8544.44	4.05	P, PCTR (PC_3)
Mg II	9246.76	4.15	P
Mg II	10917.27	4.15	P
Mg II	10918.34	4.15	P
S II	912.74	4.25	P
S II	1259.52	4.25	P
C II	1036.34	4.40	P
C II	2748.09	4.40	P
C II	4268.46	4.40	P
C II	6579.87	4.40	P
C II	6584.70	4.40	P
O II	537.83	4.45	P
O II	718.50	4.45	P, PCTR (PC_3)
O II	1128.07	4.45	P
O II	7320.94	4.45	P
O II	7332.76	4.45	P
N II	1083.99	4.45	P
He II	256.32	4.70	P, C, PCTR (PC_3)
He II	303.78	4.70	P, C, PCTR (PC_3)
S III	1190.20	4.70	P
Si III	1206.50	4.70	P
Si III	1301.15	4.70	P
Si III	1312.59	4.70	P
C III	977.02	4.85	P
N III	686.34	4.85	P
N III	991.58	4.85	P
C III	4648.72	4.85	P
C III	4651.55	4.85	P
O III	599.59	4.90	P, PCTR (PC_3)
O III	5008.24	4.90	P
O III	702.90	4.90	P
Fe V	3892.38	4.95	P
S IV	750.22	5.00	P
N IV	765.15	5.15	P, PCTR (PC_3)
O IV	553.33	5.15	P
O IV	554.51	5.15	P, PCTR (PC_3)
O IV	609.83	5.15	P
O IV	787.71	5.15	P
O IV	790.20	5.15	P
O IV	1399.78	5.15	P
O IV	1401.16	5.15	P
O V	629.73	5.35	PCTR (PC_4)
O VI	1031.91	5.45	C, PCTR (PC_4)
O VI	1037.61	5.45	C, PCTR (PC_4)
Fe VIII	168.17	5.65	PCTR (PC_4)
Mg VI	1190.12	5.65	PCTR (PC_4)
Ne VIII	770.43	5.80	C, PCTR (PC_4)
Ne VIII	780.39	5.80	C, PCTR (PC_4)
Fe IX	171.07	5.85	C, PCTR (PC_4)
Fe X	6376.29	6.05	C, PCTR (PC_4)
S IX	12523.48	6.05	C
Fe XI	7894.03	6.12	C
Si X	14304.72	6.15	C
Fe XII	186.89	6.20	C
Fe XII	195.12	6.20	C
Fe XIII	3388.91	6.25	C
Fe XIII	10749.11	6.25	C
Fe XIII	10800.77	6.25	C
Fe XIV	5304.48	6.30	C
Fe XV	7062.15	6.35	C
Ar XI	6918.02	6.68	C

Final Remarks

- We envision the lines will **facilitate complementary observations** between future instruments
- The recommended lines can be useful to **build comprehensive use-cases** with upcoming instruments available to study CMEs
- CME components can by studied with different instruments which can be combined to:
  - **study early stages of plasma evolution** with remote sensing observations
  - **connect with *in situ* observation on PSP and SO** while in quadrature with the earth

1. Rivera, Y. J., Landi, E., Lepri, S. T., & Gilbert, J. A., 2019a, 583 The Astrophysical Journal, 874, 164
2. Rivera, Y. J., Landi, E., Lepri, S. T., 2019b, The Astrophysical Journal Supplement Series, 243, 34

Thank you!

Table 1. Recommended lines above 1 phot cm^{-2} s^{-1} $arcsec^{-2}$.

Ion	λ (Å)	Log T (K)	Plasma Structure
H I (Ly-β)	1025.72	–	P
H I (Ly-α)	1215.67	–	P
H I (Hβ)	4862.73	–	P
H I (Hα)	6564.72	–	P
He I	4472.73	–	P
He I	5877.25	–	P
He I	7067.14	–	P
He I	10833.31	–	P
Ca II	3934.78	4.05	P
Ca II	8544.44	4.05	P, PCTR (PC_3)
Mg II	9246.76	4.15	P
Mg II	10917.27	4.15	P
Mg II	10918.34	4.15	P
S II	912.74	4.25	P
S II	1259.52	4.25	P
C II	1036.34	4.40	P
C II	2748.09	4.40	P
C II	4268.46	4.40	P
C II	6579.87	4.40	P
C II	6584.70	4.40	P
O II	537.83	4.45	P
O II	718.50	4.45	P, PCTR (PC_3)
O II	1128.07	4.45	P
O II	7320.94	4.45	P
O II	7332.76	4.45	P
N II	1083.99	4.45	P
He II	256.32	4.70	P, C, PCTR (PC_3)
He II	303.78	4.70	P, C, PCTR (PC_3)
S III	1190.20	4.70	P
Si III	1206.50	4.70	P
Si III	1301.15	4.70	P
Si III	1312.59	4.70	P
C III	977.02	4.85	P
N III	686.34	4.85	P
N III	991.58	4.85	P
C III	4648.72	4.85	P
C III	4651.55	4.85	P
O III	599.59	4.90	P, PCTR (PC_3)
O III	5008.24	4.90	P
O III	702.90	4.90	P
Fe V	3892.38	4.95	P
S IV	750.22	5.00	P
N IV	765.15	5.15	P, PCTR (PC_3)
O IV	553.33	5.15	P
O IV	554.51	5.15	P, PCTR (PC_3)
O IV	609.83	5.15	P
O IV	787.71	5.15	P
O IV	790.20	5.15	P
O IV	1399.78	5.15	P
O IV	1401.16	5.15	P
O V	629.73	5.35	PCTR (PC_4)
O VI	1031.91	5.45	C, PCTR (PC_4)
O VI	1037.61	5.45	C, PCTR (PC_4)
Fe VIII	168.17	5.65	PCTR (PC_4)
Mg VI	1190.12	5.65	PCTR (PC_4)
Ne VIII	770.43	5.80	C, PCTR (PC_4)
Ne VIII	780.39	5.80	C, PCTR (PC_4)
Fe IX	171.07	5.85	C, PCTR (PC_4)
Fe X	6376.29	6.05	C, PCTR (PC_4)
S IX	12523.48	6.05	C
Fe XI	7894.03	6.12	C
Si X	14304.72	6.15	C
Fe XII	186.89	6.20	C
Fe XII	195.12	6.20	C
Fe XIII	3388.91	6.25	C
Fe XIII	10749.11	6.25	C
Fe XIII	10800.77	6.25	C
Fe XIV	5304.48	6.30	C
Fe XV	7062.15	6.35	C
Ar XI	6918.02	6.68	C

CME from previous study

- Filament eruption, January 5th 2005
- Halo CME
- Acceleration = 15 km/s^2, velocity (at $30R_{sun}$) = 892 km/s
- B-class flare

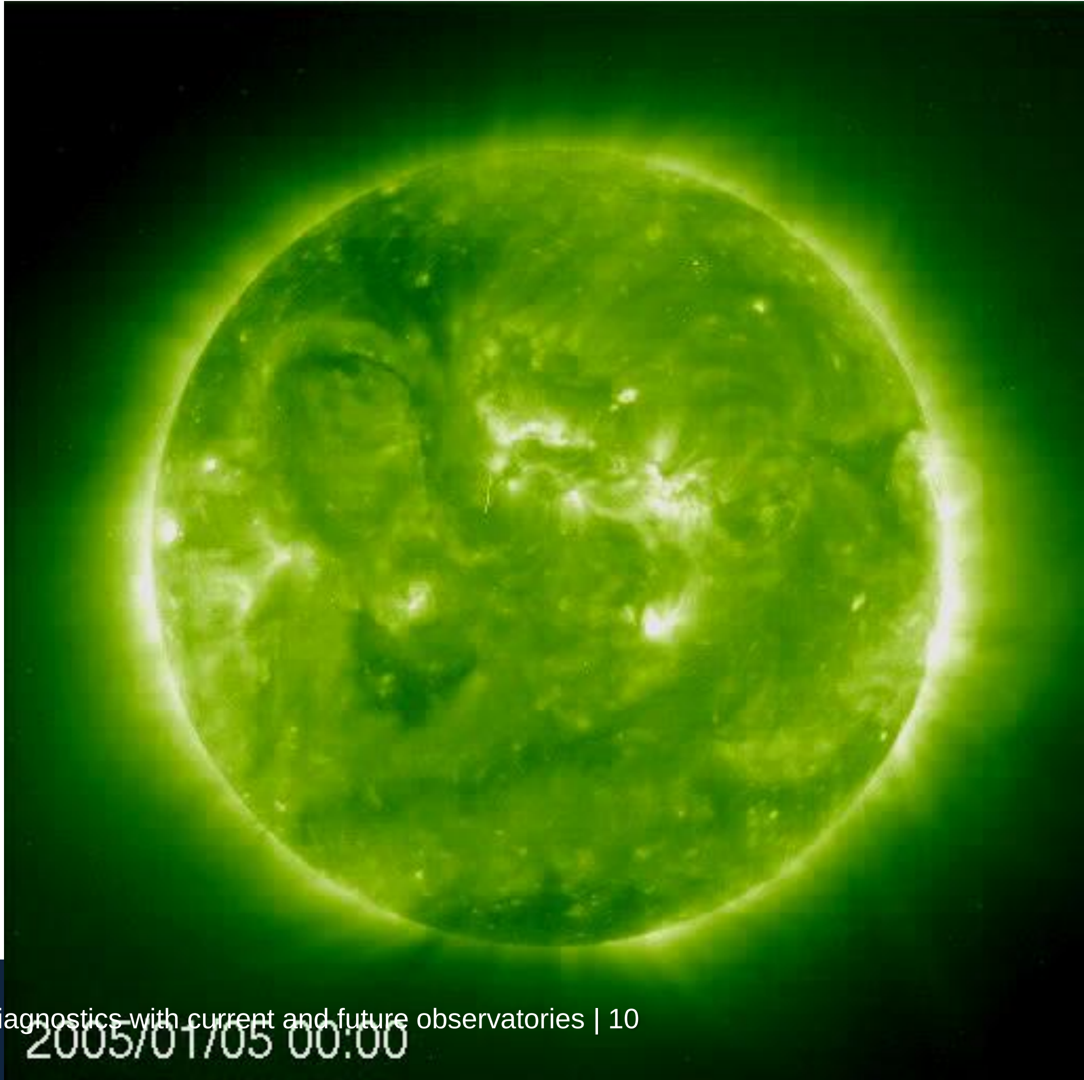

Ion Freeze-in Process

- Freeze-in process undergone by ions (Hundhausen et al. 1968)
  - Rapid decrease in density diminishes the ionization and recombination processes in the plasma
  - Ionization level is unchanged beyond the freeze-in height and retains the history of thermal evolution
  - Freeze-in heights:
    - Heights can vary even within the same species
    - Sensitive to local density, temperature, velocity

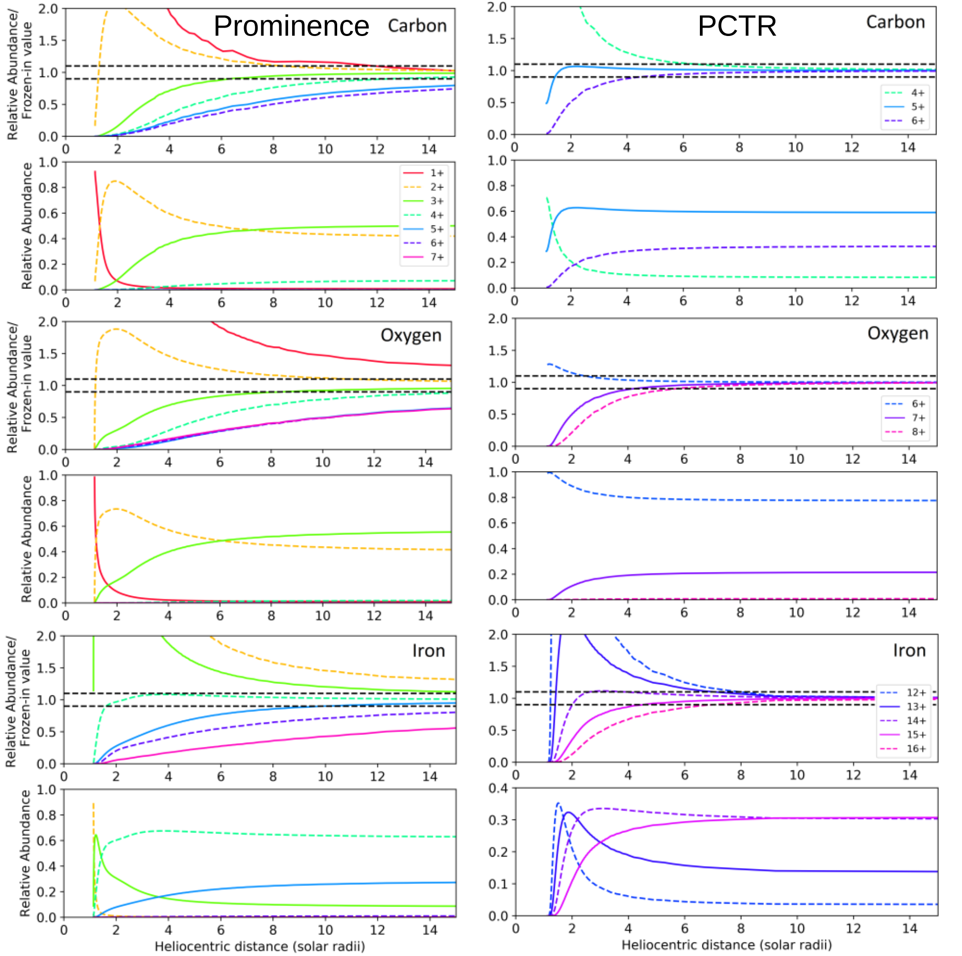

Rivera et al. 2019

Ions that **maintain equilibrium** during the eruption – lines are ***excellent*** candidates for plasma diagnostics

Ions are **out of equilibrium** during the radial evolution – multiple lines from the same ion can still provide diagnostics

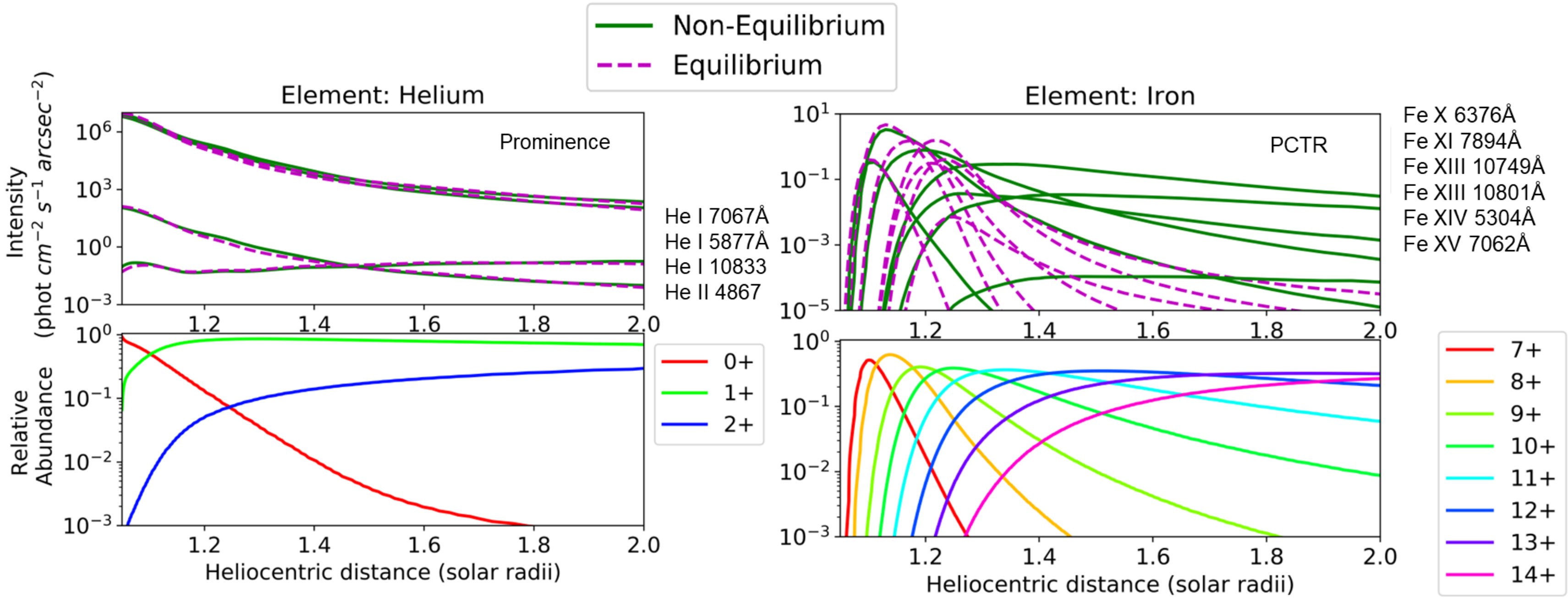

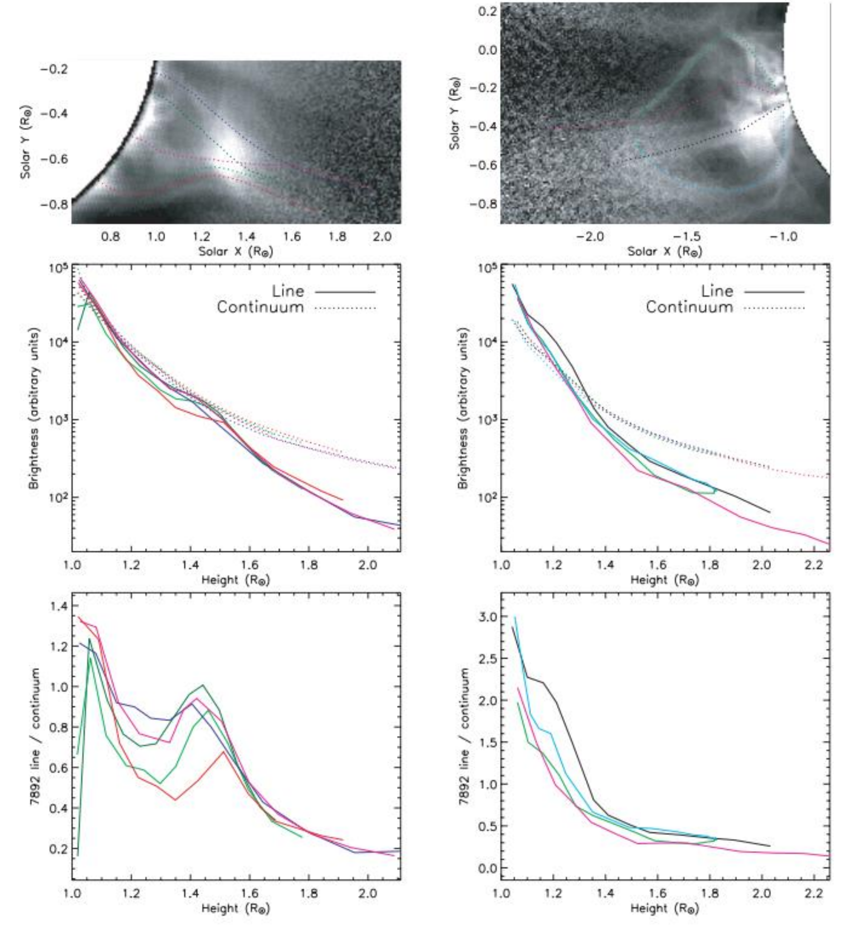

Habbal et al. 2007

Michigan Ionization Code

- The MIC is solves a time-dependent ionization equation that governs the evolution of ions in the plasma as they propagate from the Sun (Landi et al. 2012)
- Ionization/recombination processes: excitation-autoionization, dielectric recombination, collisional ionization, radiative recombination and includes the effects of EUV and X-ray photoionization.
- Main inputs:
  - Electron density
  - Electron temperature
  - Bulk flow
- Assumptions:
  - Local Thermodynamic equilibrium at boundary
  - Electron velocity Maxwellian distribution
  - Ions all moving at the same velocity, no differential flow

Sources

$$\frac{dy_i}{dt} = n_e \left[y_{i-1} I_{i-1}(T_e) + y_{i+1} R_{i+1}(T_e) \right] + y_{i-1} P_{i-1} - y_i \left[n_e \left(I_i(T_e) + R_i(T_e) \right) + P_i \right]$$

Sinks

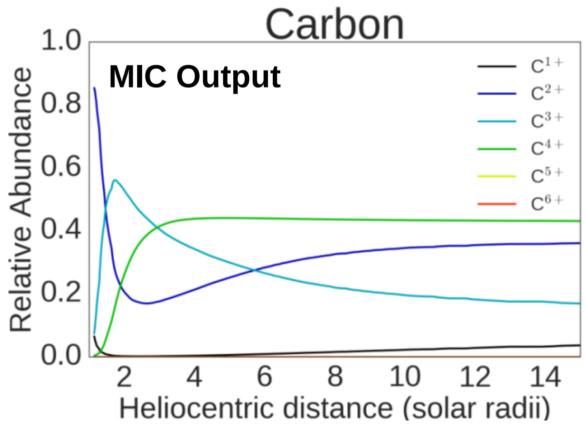

$$P_i = \int_{\nu_i}^{\infty} \frac{4\pi J(\nu) \sigma_i(\nu)}{h\nu} d\nu$$

Interplanetary CME event

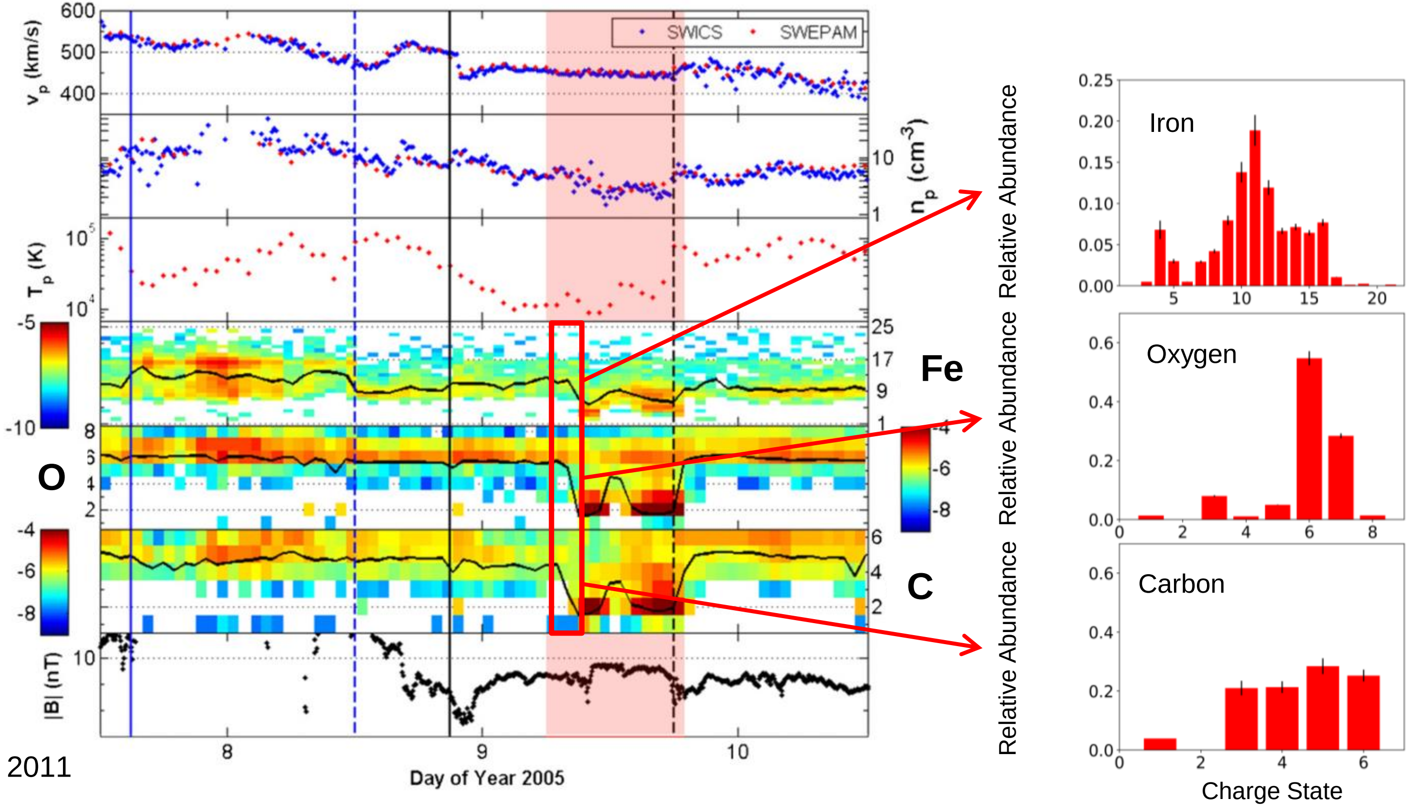

Gilbert et al. 2011

Search Algorithm

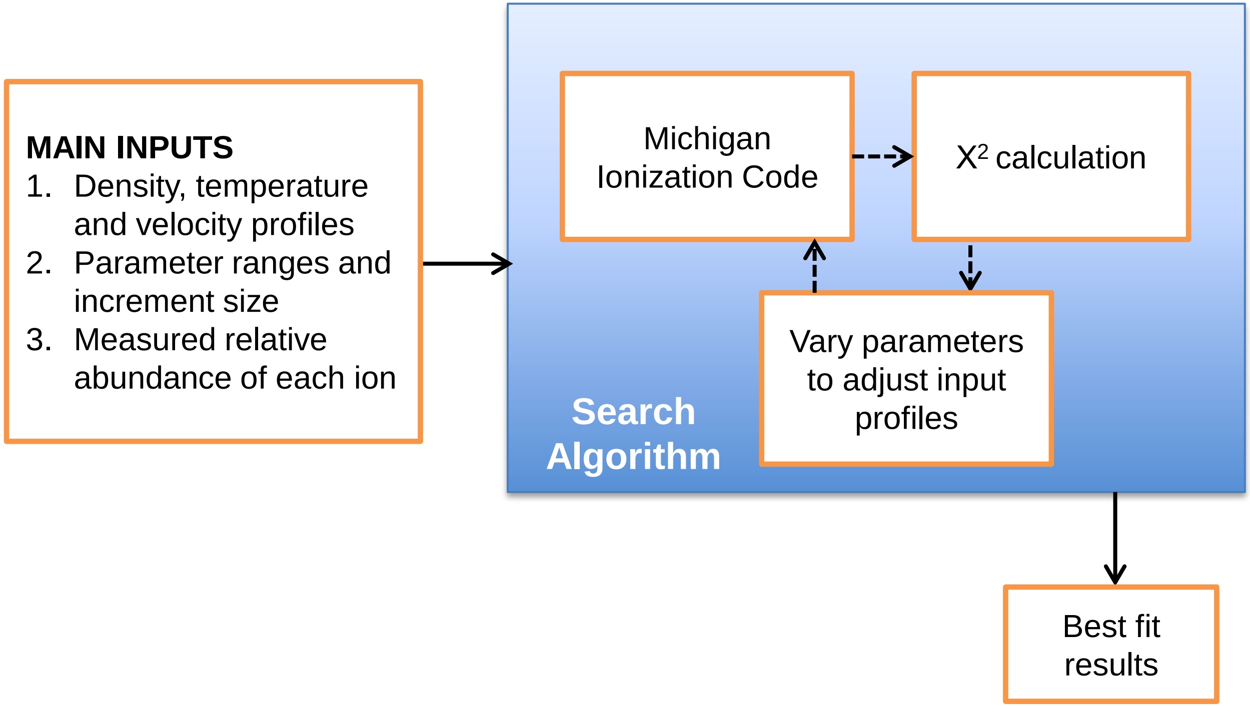

Final Distributions

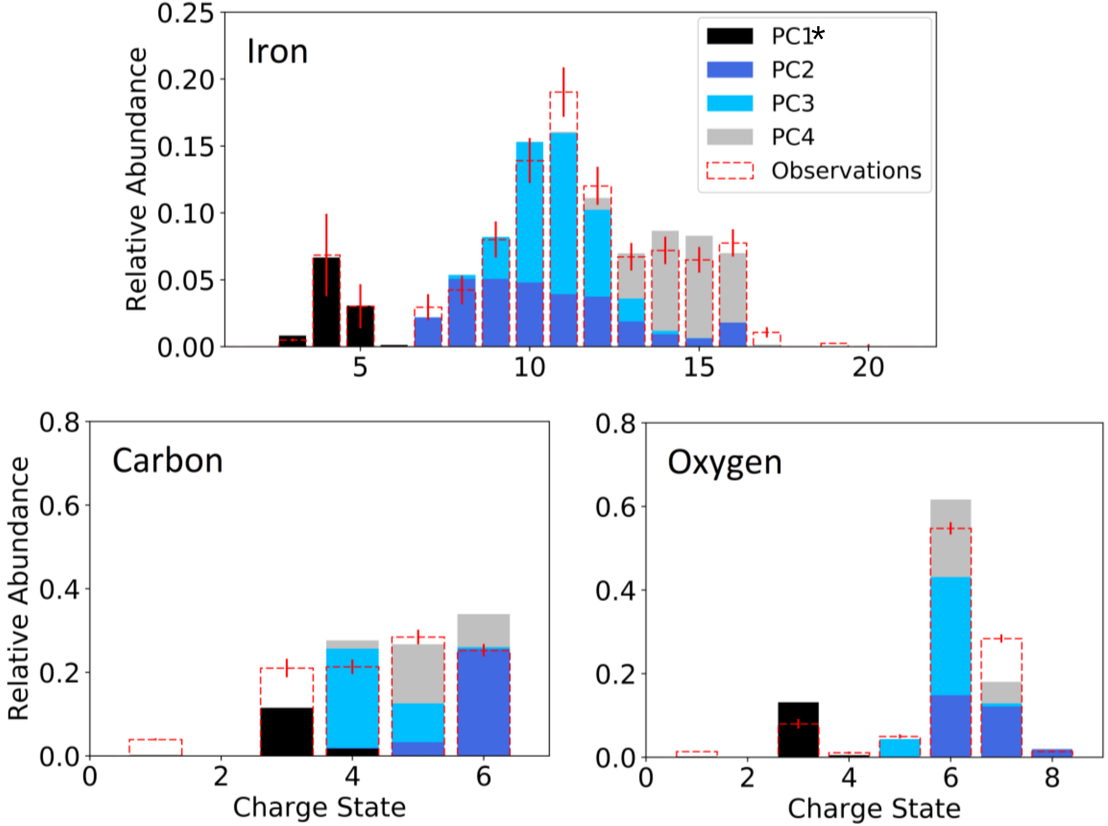

χ^2 =0.304, 95% confidence level

*Plasma Component (PC)

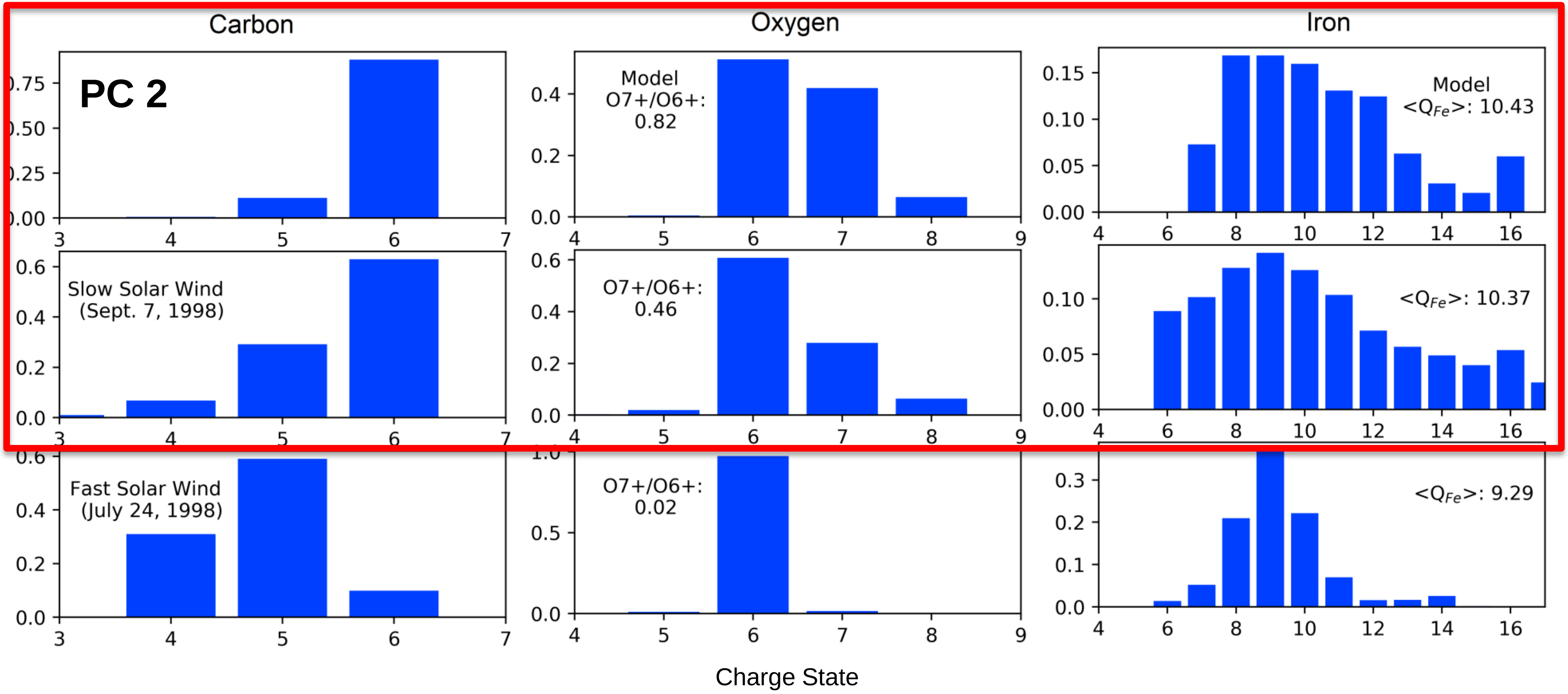
Carbon
Oxygen
Iron
PC 2
Model
O7+/O6+:
0.82
Model
<Q_Fe>: 10.43
Slow Solar Wind
(Sept. 7, 1998)
O7+/O6+:
0.46
<Q_Fe>: 10.37
Fast Solar Wind
(July 24, 1998)
O7+/O6+:
0.02
<Q_Fe>: 9.29
Charge State

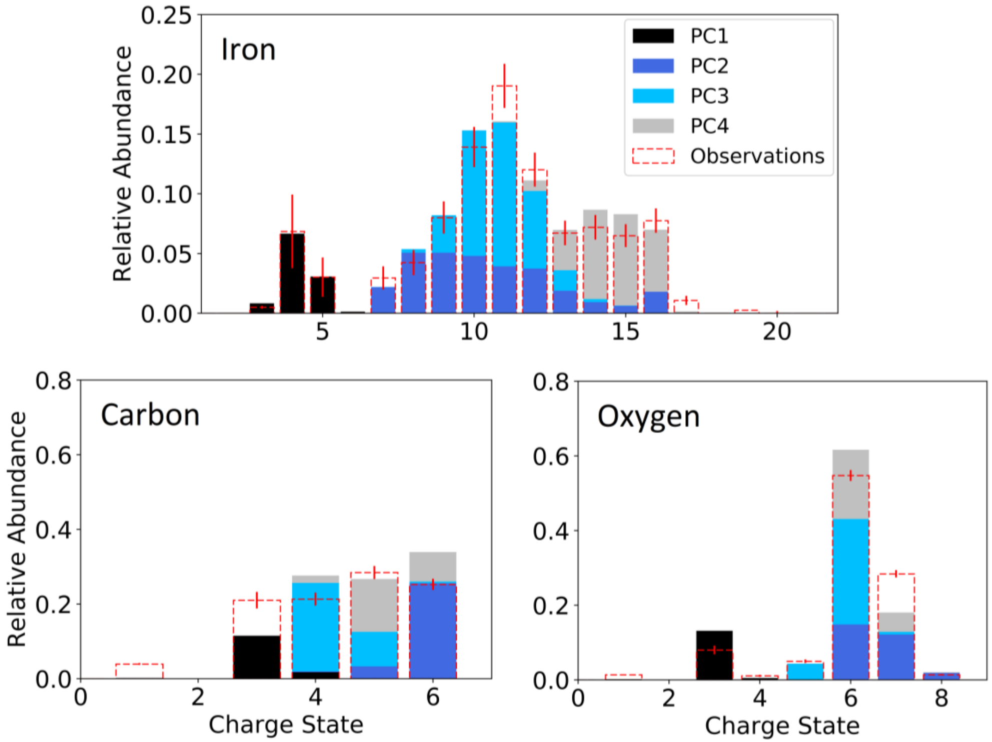

$$\mathrm{Fe}: 0.10PC_1 + 0.33PC_2 + 0.33PC_3 + 0.24PC_4$$

$$\mathrm{C\text{-}O}: 0.28PC_1 + 0.26PC_2 + 0.26PC_3 + 0.20PC_4$$

Plasma Composition

Ratio of absolute abundances to photospheric values in each PC.

PC	Fe	C	O
1	1.08±0.25	0.91±0.35	1.28±0.21
2 & 3	3.56±0.84	0.85±0.32	1.19±0.20
4	2.59±0.61	0.65±0.25	0.92±0.15

- Values computed as: $(X/H)/(X/H)_{phot}$ where $(X/H)_{phot}$ taken from Asplund et al. 2009
- Plasma Composition:
  - PC 1 – photospheric abundances
  - PC 2-4 – coronal abundances
- Variation in temporal FIP evolution? Can we track this in a newly formed filament to observe FIP evolution with DKIST?

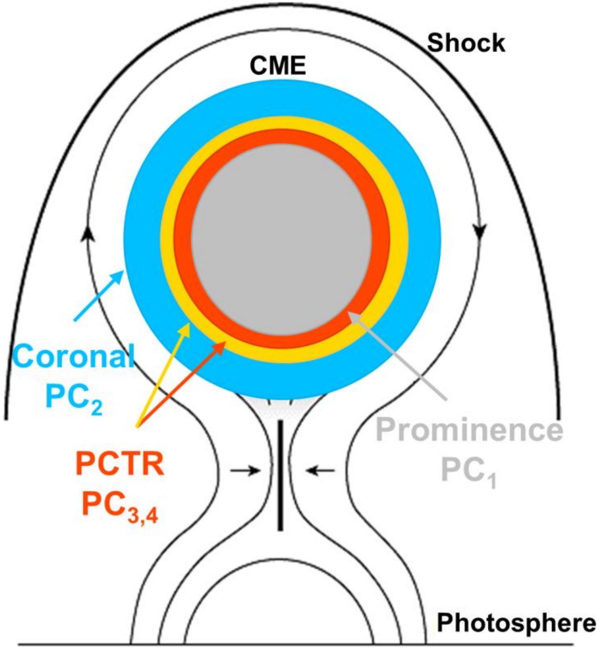

PC 1 (filament)

- Freeze-in distances between components vary:
  - PC 1: 2-25Rs
  - PC 2-4: 2-10Rs
- PC1 ions are active during the heating phase but are able to survive. Why are they so few in situ observations?
- Have potential to be continuously ionized farther from the Sun

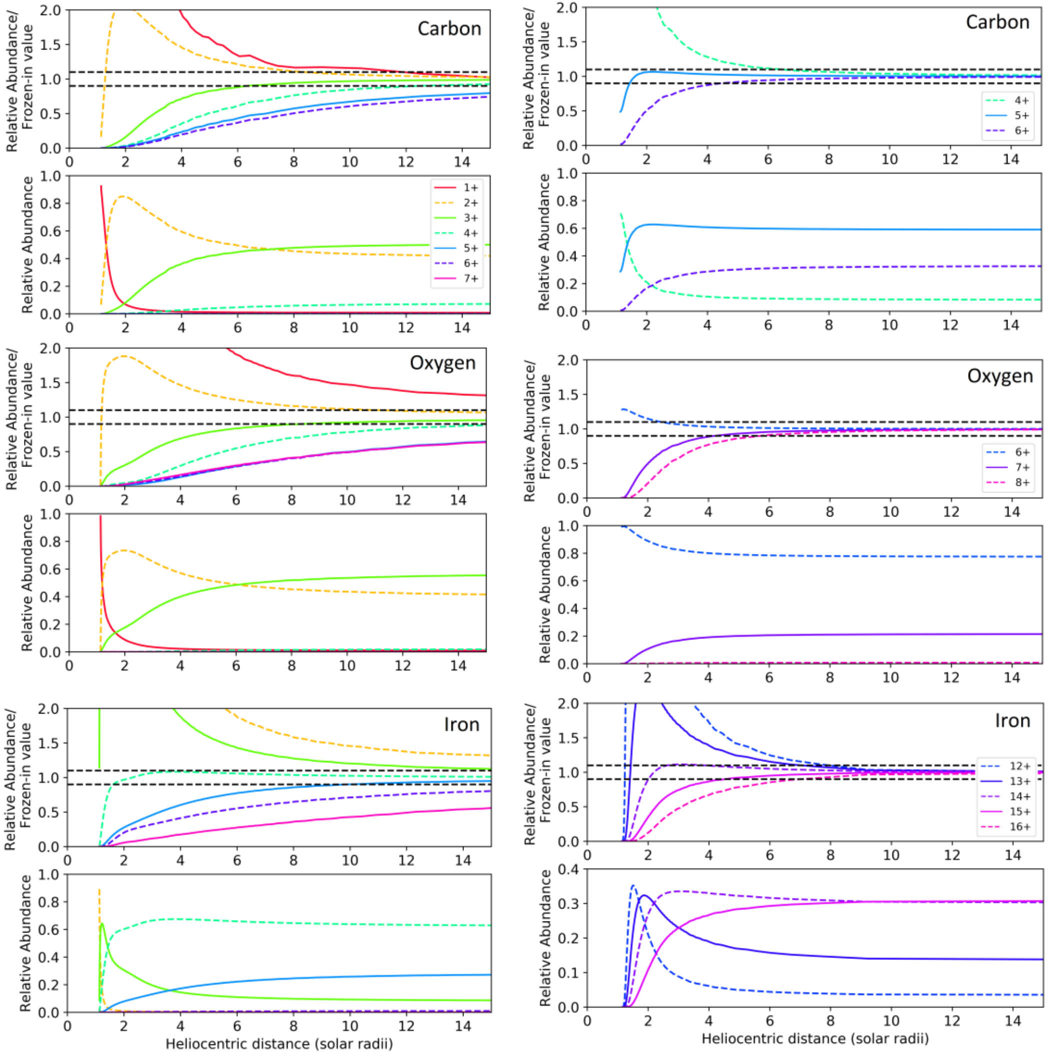

PC 4 (PCTR)